JMEPEG (2024) 33:7596–7601
https://doi.org/10.1007/s11665-024-09401-x

©ASM International
1059-9495/$19.00

ORIGINAL RESEARCH ARTICLE

Assessment of Residual Stress Behavior and Material Properties in Steels Produced via Oxynitrocarburized Metal Injection Molding

Jorge Luis Braz Medeiros, Luciano Volcanoglo Biehl, Carlos Otávio Damas Martins, Diego Augusto de Jesus Pacheco, José de Souza, and Afonso Reguly

Submitted: 21 June 2023 / Revised: 27 February 2024 / Accepted: 29 February 2024 / Published online: 1 April 2024

By combining the formability of injection-molded polymers with a wide range of metal options, metal injection molding (MIM) allows for manufacturing metallic components with small dimensions and complex geometries. However, steels produced through this process often exhibit higher porosity compared to conventional methods. This article aims to fill this gap by developing a thermochemical oxynitrocarburizing treatment cycle applied to the austenitic stainless steel Catamold 316L. The developed treatment analyzes the diffusion kinetics, mechanical properties, and metallurgical behavior. The oxynitrocarburizing treatment was carried out at a temperature of 570 °C for varying durations of 30, 60, and 120 min. The findings showed that surface microhardness significantly increased, and corrosion resistance improved due to the ceramic behavior of the Epsolon composite and the formation of magnetite, compared to the sintered material. The study reveals a substantial rise in residual compressive stresses of up to − 2790 MPa on the sample surface. The residual stress values and the elevated surface microhardness are highly beneficial for improving the tribological properties of Catamold 316L steel produced by the MIM process. The study suggests that using ionic oxynitrocarburizing in salt baths presents an alternative to plasma processes for treating Catamold 316L steel, providing improved diffusion of nitrogen and carbon.

Keywords manufacturing process, material properties, metal injection molding, oxynitrocarburizing, residual strees, 316L

1. Introduction

The austenitic stainless-steel class 316L is known for its favorable characteristics, including high ductility, superior corrosion resistance due to its low carbon content preventing sensitization, and excellent performance in cryogenic environments (Ref 1-3). In recent years, the metal injection molding (MIM) process has gained prominence, enabling the production of components with intricate geometries, small dimensions, and large production volumes. This powder metallurgy technology employs an injection method to process a mixture of metallic powder and polymeric binders, resulting in green parts with relatively low mechanical strength (Ref 4, 5).

These green parts produced through the MIM process undergo debinding processes to remove the binding polymers. Subsequently, the pieces are sintered either in vacuum furnaces or in a controlled atmosphere. During sintering, the parts can experience a volumetric contraction of approximately 20-30%, achieving densities ranging from 99 to 100% of the final steel density (Ref 6, 7). The industrial application of MIM can benefit different stainless steels, such as Catamold 316L. In this regard, the application of Catamold 316L steel finds utility in various fields, such as medicine and electronic cryogenics (Ref 6-8). However, austenitic stainless steels like Catamold 316L face limitations in terms of their mechanical strength and tribological properties, as their hardening mechanisms rely solely on plastic deformation (Ref 9). Previous studies exploring the application of the plasma nitriding process have demonstrated positive effects on surface microhardness, fatigue life through the generation of compressive stresses, and corrosion resistance by forming expanded austenite (Ref 8, 9).

In addition to the challenges posed by equipment costs and operational issues, such as the presence of a hollow cathode and variations in heating conditions, complex geometries of parts can further complicate the control of compound layers and diffusion. To overcome these challenges, this research proposes ionic oxynitrocarburizing in salt baths as an alternative to plasma processes. The method involved the introduction of approximately 3% cyanide into the liquid bath, which, upon dissociation, facilitates the diffusion of nitrogen and carbon

This invited article is part of a special topical issue of the Journal of Materials Engineering and Performance on Residual Stress Analysis: Measurement, Effects, and Control. The issue was organized by Rajan Bhambroo, Tenneco, Inc.; Lesley Frame, University of Connecticut; Andrew Payzant, Oak Ridge National Laboratory; and James Pineault, Proto Manufacturing on behalf of the ASM Residual Stress Technical Committee.

Jorge Luis Braz Medeiros, Luciano Volcanoglo Biehl, and **José de Souza**, Federal University of Rio Grande, Rio Grande, Brazil; **Carlos Otávio Damas Martins**, Federal University of Sergipe, São Cristóvão, Brazil; **Diego Augusto de Jesus Pacheco**, Aarhus University, Aarhus, Denmark; and **Afonso Reguly**, Universidade Federal do Rio Grande do Sul, Porto Alegre, Brazil. Contact e-mail: diego@btech.au.dk.

(Ref 10, 11). The degradation of the passivated Cr_2O_3 layer, caused by the oxygen source, promotes the diffusion process. During the nitriding process, a single-phase compound layer of $Fe_{2-3}N$ (ε) is formed, reducing the risk of embrittlement in polyphase layers (Ref 13, 14). Subsequently, the oxidation process contributes to the sealing of the compound layer, resulting in magnetite (Fe_3O_4) formation that significantly enhances corrosion resistance. It is assumed, therefore, that adopting this ionic oxynitrocarburizing method can better address the challenges associated with complex geometries.

The research conducted in this study involved a specific cycle comprising nitriding, oxidation, ceramic microchip polishing, and subsequent oxidation. Specifically, the primary objective of this study is to address knowledge gaps on the diffusion process in Catamold 316L MIM steels, which exhibit higher porosity levels than conventional steels. Another important aspect of the method developed is the investigation of the behavior of the composite layer, diffusion, corrosion resistance, and residual stresses that arise from the application of the oxynitrocarburizing process in complex geometries.

This research establishes a scientific contribution to the field by mapping the behavior of the substrate, particularly concerning the presence of precipitates that may form along the austenitic grain boundaries. The understanding of diffusion kinetics and their correlation with residual surface stresses, as determined through XRD tests, can open up new possibilities for applying this thermochemical cycle in steels with tribological limitations. Through our research, valuable empirical insights can be gained to enhance the performance and applicability of these steels in the industry. This study also contributes to complementing the previous literature (Ref 15-21).

2. Methods

The raw material utilized in this research was Catamold 316L Basf. To obtain the samples, nine cylindrical specimens with a diameter of 12 mm and a height of 5 mm were produced using an Arbor injector at a temperature of 120 °C, referred to as green samples. The polymer binder (debinding) was removed in a Cremer oven, employing nitric acid vapor with a purity of 99.99%.

Following this, the samples underwent sintering in a controlled atmosphere furnace utilizing 100% hydrogen. The chemical composition of the samples was analyzed using a Foutrin optical emission spectrometer. Finally, the sintered samples were subjected to the thermochemical oxynitrocarburizing treatment.

The experimental cycle commenced by preheating the samples in an atmosphere-free oven at 300 °C for 30 min. Subsequently, the specimens were immersed in the TF1 nitriding bath containing aerated cyanate at temperatures of 570 °C for 30, 60, and 120 min. Following the nitriding stage, the samples underwent oxidation in the AB1 bath for 15 min, followed by rapid cooling in water at room temperature. The oxidized samples were then subjected to glass microsphere blasting, submerged once again in the AB1 bath for 15 min, and cooled in water at room temperature.

Subsequently, the oxynitrocarburized samples were characterized using different methods. Optical microscopy analysis was conducted using an Olympus GX 51S microscope, while scanning electron microscopy (SEM) was performed using a Jeol JSM-6610LV instrument. Energy-dispersive spectroscopy (EDS) microprobe analysis was also carried out. Vickers microhardness measurements were obtained using a Shimadzu HMV 2 T equipment.

The electrochemical tests were conducted on an Autolab PGSTAT302N potentiostat using a three-electrode electrochemical cell, using a saturated calomel electrode as a reference and a platinum rod as a counter electrode. The electrolyte used was a 0.1 mol L^{-1} NaCl solution, with PH 5.7 at a temperature of 22 °C. The OCP open circuit potential was monitored for 3600 seconds, followed by cyclic potentiodynamic polarization, starting from 300 mV cathodic with respect to the OCP to 3000 mV anodic with respect to the OCP under a scan rate of 1 mV S^{-1}. The assay was set to reverse the direction of the scan when the run reached 0.01 B C^{-2}.

The x-ray diffraction (XRD) analyses were conducted directly on the sample surface without prior preparation. XRD analysis was performed using a GE Seifert Charon XRD M apparatus with monochromatic CrKα radiation. The apparatus operated at a voltage of 40 kV, a current density of 30 mA, and a step size of 0.02° (2θ) per second. The following section shows the results obtained.

3. Results and Discussion

Close to the surface, the analysis revealed the formation of a layer of compounds exhibiting darkening on the external side of the cross section. It was verified directly by optical microscopy and scanning electron microscopy. A compound layer (white) and a diffusion layer were observed. The austenitic substrate did not exhibit any microstructural evidence of sensitization. Figure 1 illustrates the darkened compound layer near the surface, the compound layer (white), and the diffusion layer, indicating the rupture of the Cr_2O_3 film and the occurrence of diffusion. The oxidation behavior of the composite layer was similar to that observed in previous studies on AISI 304L austenitic stainless steel following the degradation of the passivated film (Ref 5, 6, 11, 12).

In steels produced using MIM technology, the degradation of the Cr_2O_3 layer is intensified due to the increased porosity, resulting in micro-tensions between the pores and the passivated surface film (Ref 5, 6, 11, 12). During the experiments, no signs of erosion or rupture were observed in the composite layer, which exhibits a brittle behavior (Ref 5, 6). The surface condition of the studied samples, being raw from sintering, also contributes to the initial degradation of the Cr_2O_3 layer. This phenomenon hinders the formation of oxide films with reduced and nonuniform thickness (Ref 5, 6). Moreover, SEM/EDS analyses confirmed the presence of a composite layer with a single-phase morphology, as depicted in Fig. 1(d). Furthermore, all samples subjected to different oxy-nitrocarburizing times exhibited a uniform diffusion layer without significant variations.

The EDS microprobe analysis of the diffusion zone revealed that the main mechanism involved the solid solution of nitrogen in austenite and a reduced presence of CrN precipitates (Ref 3, 4). Figure 2 illustrates the compound layer and the diffusion layer, visible in (a) and (b) of the EDS microprobe peaks, within the compound layer and beneath the diffusion bed.

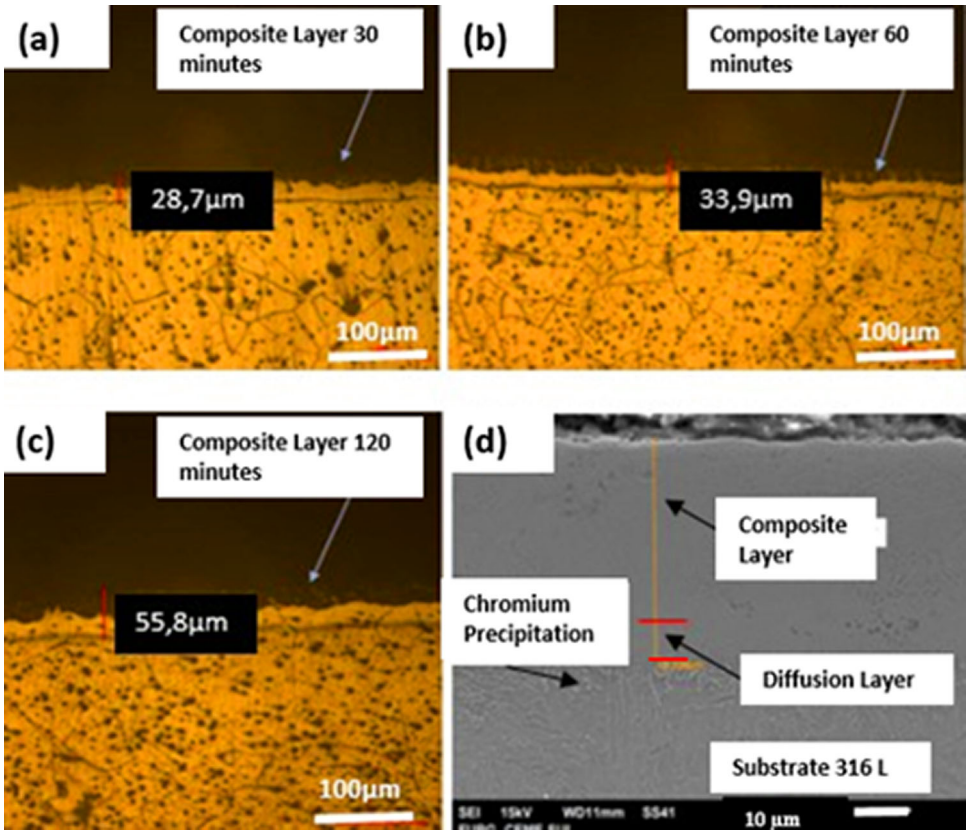

Fig. 1 Layer of compounds in optical microscopy after oxynitrocarburizing for 30 min (a), 60 min (b), 120 min (c) and morphology in the 120-min cycle in SEM (d)

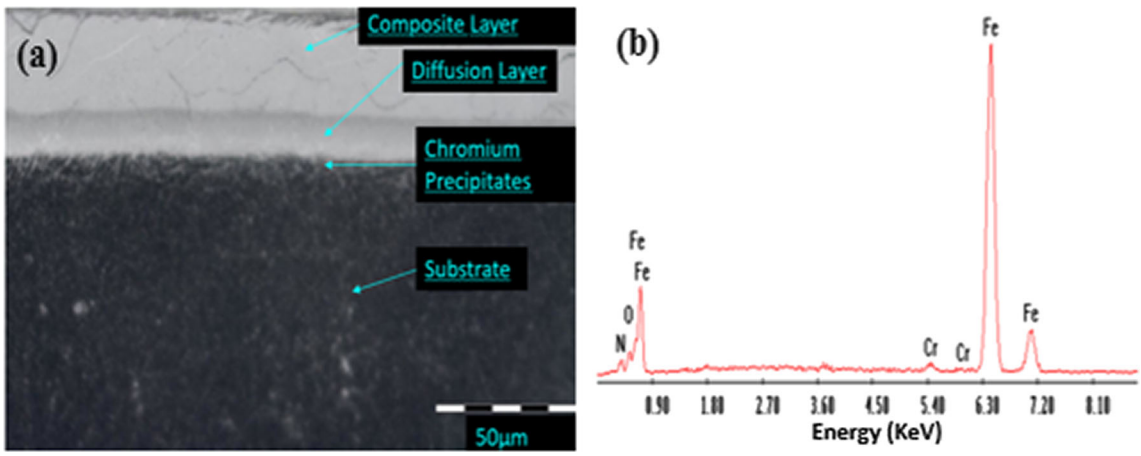

Fig. 2 Identification of the compound, diffusion, and substrate layers in (a). The qualitative analysis obtained in the EDS test is presented in (b)

The formation of the diffusion layer following the composite layer is intensified by the presence of porosities and the permeability of magnetite to nitrogen (Ref 6). Additionally, the presence of the ε-Fe3N monophasic compound layer facilitates nitrogen diffusion (Ref 6). However, the presence of expanded austenite was not detected, which can be attributed to the long cycles applied and the surface irregularity of the samples in the raw sintered condition, without passivation, leading to the heterogeneous behavior of Cr_2O_3 (Ref 6).

Table 1 presents the depths of the compound layers and shows the corresponding average microhardness values observed after oxynitrocarburizing for durations of 30, 45, and 60 min. The outcomes indicated an increase in the depths of the compound layers as the nitrocarburizing time increased, although no direct correlation was observed. This suggests that the kinetic effect of the process is reduced with longer durations due to barriers formed by nitrogen supersaturation, the presence of magnetite, and other barriers within the austenite (Ref 4, 5).

Table 1 Values of composite layer and superficial microhardness of the samples

Composite layer, min	Average depth, μm	Average microhardness $HV_{0.05}$
30	28.7	1335
60	33.9	1596
120	55.8	1443

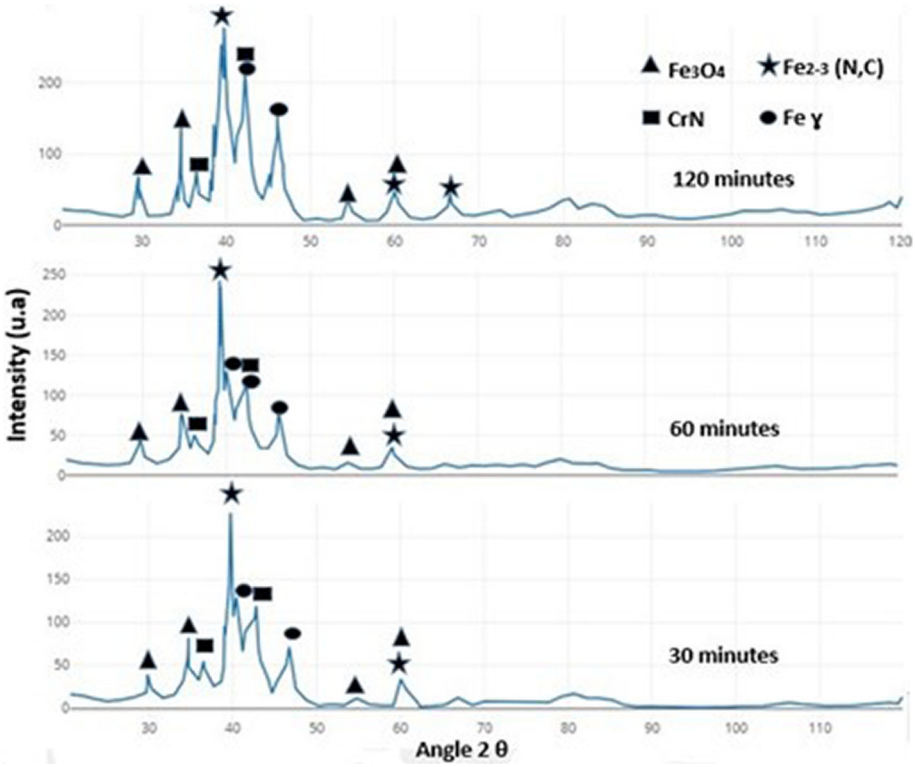

Fig. 3 Results of the x-ray diffraction of the oxynitrocarburized samples

Figure 3 illustrates the x-ray diffraction (XRD) profiles of the base material and the oxynitrocarburized samples obtained at 30, 60, and 120 min. The XRD analysis revealed the presence of prominent peaks corresponding to CrN, Fe_3O_4, $Fe_{2-3}N$, and Gamma Iron. Nonetheless, no evidence of the gamma line or expanded austenite layer was detected. This suggests that the formed compound layer is predominantly monophasic, which contributes to its enhanced stability and reduced fragility (Ref 5-8, 18). The presence of Fe_3O_4 peaks potentially enhances the corrosion resistance of stainless steel. Additionally, the low carbon content in Catamold 316L steel minimizes the formation of carbon-based precipitates (Ref 5).

The Vickers microhardness profile (HV 0.05) results revealed that the effective diffusion layer thickness was 0.1 mm for the sample subjected to a 30-min thermochemical treatment, 0.15 mm for the 60-min treatment, and 0.22 mm for the 120-min treatment. These findings showed that the microhardness was significantly higher near the surface, gradually decreasing toward the substrate. This behavior can be attributed to the austenitic nature of the studied steel, which relies on plastic deformation as its primary hardening mechanism. However, the absence of a distinct transition zone in the oxynitrocarbonized layer may make it susceptible to chipping.

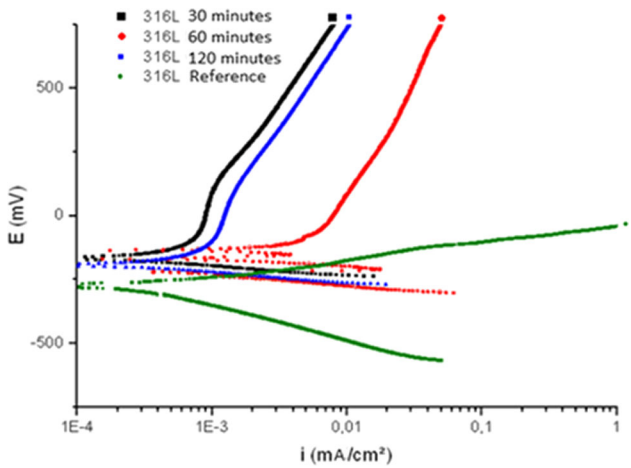

Fig. 4 Anodic potentiodynamic polarization curves of the samples

Figure 4 displays the anodic potentiodynamic polarization curves of the samples in the initial sintered condition, considered as the reference, and after the application of oxynitrocarbonation for 30, 60, and 120 min.

In all the experiments performed, the oxynitrocarburized samples exhibited superior corrosion resistance compared to the sintered base metal. Among the tested samples, the ones nitrided for 30 min, followed by a 120-min thermochemical treatment, demonstrated the best resistance to corrosion and passive film formation. However, it is noteworthy that the behavior of the oxynitrocarburized sample treated for 60 min differed from the others. The results indicated that this particular sample exhibited subsurface chromium segregation, which seemingly contributed to the heterogeneity of the composite layer and the sealing of magnetite formation. The effectiveness of the applied cycles is evident in the formation of a protective film that enhances the material's performance in critical environments, even in sintered condition (Ref 7).

The analysis of residual stresses resulting from the oxynitrocarburizing cycle is crucial for steels produced through the MIM process. Austenitic stainless steels like Catamold 316 L primarily rely on plastic deformation for hardening, making it challenging to generate consistent compressive stresses. XRD analysis revealed surface stress values of − 451 MPa, − 2691 MPa, and − 2769 MPa in the transverse and longitudinal directions after oxynitrocarburizing for 30, 60, and 120 min, respectively.

Figure 5 displays the average stress values in both directions. Notably, the results indicated that oxynitrocarburizing for over 60 min significantly increased compressive stresses, attributed to the presence of the Epsilon single-phase layer on the surface.

This study found that the generation of residual stresses in the oxynitrocarburizing process is influenced by the interaction of Cr nitrides and carbides with final oxidation, resulting in the formation of Fe_3O_4. Additionally, it was verified that changes in residual stress states occur due to nitrogen supersaturation, leading to a sharp transition in microhardness between the composite, diffusion, and substrate layers.

These findings align with previous research conducted on different materials using processes other than MIM (Ref 8, 19, 21). The effect of time variation was significant on the depth of the compound and diffusion layer. However, in microhardness and electrochemical tests, the data showed randomness. This condition is related to the preliminary condition of the substrate. However, the metallurgical and mechanical properties of Catamold 316L steel showed significant improvements. It is noteworthy that the effect of interstitial diffusion of nitrogen and carbon in the oxynitrocarburization process must be optimized since, in regions of reduced thickness, embrittlement may occur due to the encounter of layers (Ref 5, 6).

The paper's findings show that the inclusion of a glass microsphere blasting step between the first and second oxidations contributes to the development of a thin layer of plastic deformation, further increasing residual compressive stresses along the surface. This blasting also contributes to reducing the final roughness of the components (Ref 10, 11). The increase in layer depth directly correlates with the intensification of residual stresses, a phenomenon observed in samples subjected to nitrocarburizing for 60 and 120 min.

4. Conclusions

Based on the results and discussion of the oxynitrocarburization of Catamold 316L steel, the conclusions regarding metallurgical and mechanical properties are indicated as follows:

- The oxynitrocarburizing process resulted in the formation of a monophasic Epsilon layer of compounds in the austenitic stainless steel Catamold 316L samples. The compound layer was monophase Epsilon, which reduced the possibility of its embrittlement.
- The presence of magnetite was observed on the outer part of the composite layer. The presence of magnetite represents a factor that contributed to corrosion resistance, even with the presence of CrN in stainless steel.
- Surface microhardness values exceeded 1000 HV in all samples.
- The samples exhibited enhanced corrosion resistance in the sintered condition with subsequent oxynitrocarburizing compared to the sintered base material.
- Factors associated with diffusion kinetics related to the porosity level were not observed in the samples.
- Compressive residual stresses were detected in different regions of all samples, with values exceeding − 2000 MPa for 60 and 120 min cycles. The sample oxynitrocarburized for 60 min showed higher values of

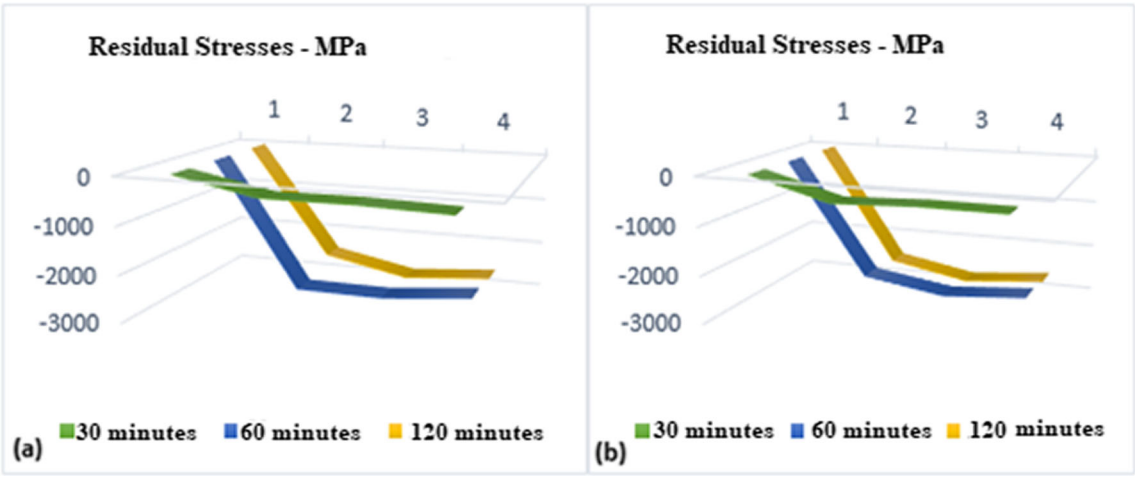

Fig. 5 Residual stresses in the longitudinal direction in (a) and Hoop in (b)

compressive residual stresses.

- The high compressive residual stress values and the surface microhardness are highly beneficial for improving the tribological properties of Catamold 316L steel produced by the MIM process.
- Using ionic oxynitrocarburizing in salt baths presents an alternative to plasma processes for treating Catamold 316L steel, providing improved diffusion of nitrogen and carbon.

References

1. C. Wang, X. Lin et al., Cryogenic Mechanical Properties of 316L Stainless Steel Fabricated by Selective Laser Melting, *Mater. Sci. Eng. A*, 2021, **815**, p 1–10.
2. F.E. Kennedy, Y. Ye, I. Baker et al., Development of a New Cryogenic Tribotester and its Application to the Study of Cryogenic Wear of AISI 316 Stainless Steel, *Wear*, 2022, **496–497**, p 1–10.
3. X. Chen, J. Li et al., Microstructure and Mechanical Properties of the Austenitic Stainless Steel 316L Fabricated by Gas Metal Arc Additive Manufacturing, *Mater. Sci. Eng. A*, 2017, **703**, p 567–577.
4. H. Ye, X.Y. Liu, and H. Hong, Fabrication of Metal Matrix Composites by Metal Injection Molding: A Review, *J. Mater. Process. Technol.*, 2008, **200**, p 12–24.
5. J.L.B. Medeiros, T.R. Strohacker, and A. Reguly, Applying Oxy-Nitrocarburizing Surface Strengthening Process to Corrosion Prevention in MIM 17-4 PH Stainless Steel, *Espacios*, 2015, **36**, p 21–26.
6. F. Lantelme, H. Groult, H. Mosqueda, P.-L. Magdinier, H. Chavanne, V. Monteux, and P. Maurin-Perrier, Salt bath thermal treating and nitriding. In: F. Lantelme, H. Groult (Eds.) *Molten Salts Chemistry: From Lab to Applications*, Oxford, 2013, pp. 101–129
7. A.P.G. Mendoza, G.V. Gutierres et al., Surface Microstructural Evolution of AISI 304 L Stainless Steel Oxynitrocarburized in a Cyanide-Free Salt Bath and its Potential Application in Solar Collectors, *Surf. Coat. Technol.*, 2018, **353**, p 190–198.
8. W.A. Monteiro, S.A. Lima Pereira, and J. Vatavuk, Nitriding Process Characterization of Cold Worked AISI 304 and 316 Austenitic Stainless Steels, *J. Metall.*, 2017, **2017**, p 1–7.
9. J. Wang, Y. Lin, J. Yan, D. Zeng, R. Huang, and Z. Hu, Modification of AISI 304 Stainless Steel Surface by the Low Temperature Complex Salt Bath Nitriding at 430 °C, *ISIJ Int.*, 2012, **52**, p 1118–1123.
10. D. Heaney, Powders for metal injection molding (MIM). In: Handbook of Metal Injection Molding MIM. Woodhead Publishing Series in Metals and Surface Engineering, pp. 45–56, 2019
11. T.H. Scheneider, L.V. Biehl, J.L.B. Medeiros, and J.D. Souza, Method for the Determination of Parameters in the Sintering Pross of Mixtures of the Elemental Powders Fe-Cr and Fe-Cr-Ni, *MethodsX*, 2019, **6**, p 1919–1924.
12. M.U. Oliveira, L.V. Biehl, J.L.B. Medeiros, C.A.O. Avellaneda, C.O.D. Martins, J.D. Souza, and F. Sporket, Manufacturing Against Corrosion: Increasing Materials Performance by the Combination of Cold Work and Heat Treatment for 6063 Aluminium Alloy, *Mater. Sci. Medziagotyra*, 2019, **26**, p 30–33.
13. R.K. Enneti, V.P. Onbattuvelli et al. Powder-binder formulation and compound manufacture in metal injection molding (MIM). In: Handbook of Metal Injection Molding MIM, p. 57–88, 2019
14. T.K. Hirsch, A.D.S. Rocha, F.D. Ramos, and T.R. Strohacher, Residual Stress-Affected Diffusion during Plasma Nitriding of Tool Steels, *Metall. Mater. A*, 2004, **35 A**, p 3523–3530.
15. K. Tkacz-Śmiech, B. Wierzba, B. Bożek, and M. Danielewski, Nitrogen Diffusion and Stresses During Expanded Austenite Formation in Nitriding, *Defect Diffus. Forum*, 2016, **371**, p 49–58.
16. J.V.P.D. Nora, J.L. BrazMedeiros, L.V. Bieh et al., The Influence of Thermal Cycles on the Performance and Spheroidization Process of SAE 8640 Steels, *J. Mater. Eng. Perform.*, 2022, **3**, p 1–9.
17. J.K. Toole, M. Burnet et al., Influences of Vanadium and Silicon on Case Hardness and Residual Stress of Nitrided Medium Carbon Steels, *Metall. Mater. A*, 2021, **2**, p 1–14.
18. E.D.R. Vieira, L.V. Biehl, J.L.B. Medeiros, V.M. Costa, and R.J. Macedo, Evaluation of the Characteristics of an AISI 1045 Steel Quenched in Different Concentration of Polymer Solutions of Polyvinylpyrrolidone, *Sci. Rep.*, 2021, **11**, p 1–8.
19. R.C.L.M. Oliveira, L.V. Biehl, J.L.B. Medeiros, D. FerreiraFilho, and J.D. Souza, Análise comparativa entre a têmpera e partição versus a têmpera e revenimento para o aço SAE 4340, *Materia*, 2019, **24**, p 1–9.
20. E.R. Vieira, L.V. Bieh, J.L.B. Medeiros, A.B. Silva, and M.S.D. Silva, Efeitos da variação da concentração de solução polimérica aquosa a base de PVP na têmpera de aço AISI 4140, *Materia*, 2019, **24**, p 1–11.
21. R. Tochetto, R. Tochetto, L.V. Biehl, J.L.B. Medeiros, and J.D. Souza, Evaluation of the Space Holders Technique Applied in Powder Metallurgy Process in the Use of Titanium as Biomaterial, *Lat. Am. Appl. Res.*, 2019, **49**, p 261–268.

Publisher's Note Springer Nature remains neutral with regard to jurisdictional claims in published maps and institutional affiliations.

Springer Nature or its licensor (e.g. a society or other partner) holds exclusive rights to this article under a publishing agreement with the author(s) or other rightsholder(s); author self-archiving of the accepted manuscript version of this article is solely governed by the terms of such publishing agreement and applicable law.